Quantum effects in thermal reaction rates at metal surfaces

Dmitriy Borodin^{a,b}*, Nils Hertl ^{a,b}, G. Barratt Park ^{a,b,c}, Michael Schwarzer ^a, Jan Fingerhut ^a, Yingqi Wang^d, Junxiang Zuo^d, Florian Nitz ^a, Georgios Skoulatakis^b, Alexander Kandratsenka^b, Daniel J. Auerbach ^b, Dirk Schwarzer^b, Hua Guo^d, Theofanis N. Kitsopoulos ^{a,b,e,f} and Alec M. Wodtke ^{a,b}**

^aInstitute for Physical Chemistry, University of Göttingen, Tammannstraße 6, 37077 Göttingen, Germany

^bDepartment of Dynamics at Surfaces, Max-Planck Institute for Multidisciplinary Sciences, am Faßberg 11, 37077 Göttingen, Germany

^eDepartment of Chemistry and Biochemistry, Texas Tech University, Box 41061, Lubbock, TX 79409-1061, USA

^dDepartment of Chemistry and Chemical Biology, University of New Mexico, Albuquerque, NM 87131, USA

^eDepartment of Chemistry, University of Crete, 71003 Heraklion, Greece,

^fInstitute of Electronic Structure and Laser, FORTH, 71110 Heraklion, Greece

Abstract

There is wide interest in developing accurate theories for predicting rates of chemical reactions occurring at metal surfaces, especially for applications in industrial catalysis. Conventional methods contain many approximations that lack experimental validation. In practice, there are few reactions where sufficiently accurate experimental data exist to even allow meaningful comparisons to theory. Here, we present experimentally derived thermal rate constants for H atom recombination on Pt single crystal surfaces, accurate enough to test established theoretical approximations. A quantum rate model is also presented, making possible a direct evaluation of the accuracy of commonly used approximations to adsorbate entropy. We find that neglecting the wave nature of adsorbed H atoms and their electronic spin-degeneracy led to $10 - 1000 \times$ overestimation of the rate constant for temperatures relevant to heterogeneous catalysis. These quantum effects are also found to be important for nanoparticle catalysts.

Main Text:

Enormous effort has gone into developing predictive theories of thermal reaction rates (1) with one goal being accurate kinetic models of heterogeneous catalysis, an industrial corner-stone of modern society (2). Modeling real catalytic reactors presents technical problems as they often involve networks of reactions (3, 4), complicating meaningful comparisons to experiment that could test a theory's assumptions. A possible solution is to compare experiment and theory using simplified model systems involving only a single elementary reaction. Unfortunately, even this comparison is seldom achieved as accurate measurements of elementary reaction rates are rare in surface chemistry (5).

Illustrative of these problems is the thermal recombination of H atoms on transition metals, leading to H_2 formation. Perhaps the simplest reaction for theoretical modeling and omnipresent as an elementary step in industrial catalysis (*e.g.* hydrogenation of unsaturated fats (*6*), ammonia synthesis (7) and electrochemical hydrogen production (8)), it is an obvious starting point for development of accurate rate theories in surface chemistry. Unfortunately, large uncertainties in the experimentally derived 2^{nd} -order rate constants arise due to difficulties in obtaining accurate initial concentrations (9). If these and other experimental problems could be overcome, this reaction would provide an ideal system for benchmarking rate theory, especially for testing approximate treatments of quantum effects.

From the study of gas-phase reactions, exact treatments of nuclear quantum effects are often considered to be unnecessary above $\sim 500 \text{ K}$ (10) and because most catalytic reactors operate at elevated temperatures, one might conclude that a classical approximation (11) or approximate ad hoc quantum treatments like harmonic transition-state theory (hTST) (12, 13), would be sufficient to model surface chemistry. But the need to go beyond hTST has been pointed out recently (14) and new methods were reported, although they also lack validation from experiment. Electron spin is another important quantum effect on surface reactions – for example, in H atom recombination, only one out of four electron spin combinations yields a stable H_2 molecule. However, the spin-degeneracy of reactants and products has – to our knowledge – never been included in calculations of reaction rates at metal surfaces.

This paper reports kinetic data for H atom recombination on both the Pt(111) and (332) surfaces obtained with Velocity Resolved Kinetics (VRK), previously used only to study 1st and pseudo-1st

order reactions on model catalysts (15, 16). For this work, we have extended VRK to the measurement of rate constants for 2^{nd} -order reactions by measuring the absolute reactant flux, which when combined with known sticking probabilities (17, 18), provides accurate initial concentrations [H]₀ and eliminates the main source of error found in previous work.

To understand the kinetics more deeply, we also constructed a quantum rate model (QRM) that accurately reproduced experimental rate constants over twelve orders of magnitude for temperatures between 250 and 1000 K with no adjustable parameters. Comparison to a corresponding classical rate model (CRM) revealed how large and crucially important quantum effects are; the classical reaction rate constants were ~20 times larger than quantum rate constants even at 1000 K with an increasing deviation at lower temperatures. For reaction at stepped surfaces, the errors were even higher. This dramatic quantum reduction of the reaction rate resulted from both the delocalization of the adsorbed H* nuclei and as well as the influence of electron spin-degeneracy.

The experiments are described in detail in the Supplementary Materials (SM). Briefly, a pulsed molecular beam, with a controlled mixture of H_2 and D_2 illuminated either a Pt(111) or (332) crystal facet, with step densities of 0.1-0.6% and 16.7%, respectively. The transient rates of HD formation were then recorded using VRK, where pulsed laser-ionization, time-of-flight mass spectrometry reports the product's mass-to-charge ratio (m/Z) and its density as a function of delay between the pulsed molecular and laser beams. Because the ions were detected with slice imaging (19, 20) yielding product velocity, we could accurately compute the transient product flux as a function of reaction time at the surface. Initial reactant concentrations are needed to obtain 2^{nd} order rate constants (Sec. S2 (a), SM). These values were obtained from the absolute flux profiles of the incident molecular beams—Section S2(b), SM—and known sticking coefficients (17, 18)—Section S3, SM. Finally, VRK data obtained at m/Z = 2, 3 & 4 led to isotopic branching fractions—Section S4, SM—from which we obtained isotope-specific rate constants.

The QRM developed in this work is an exact formulation of a thermal rate constant. It yields accurate isotope-specific thermal rates as long as one has accurate isotope-specific thermal sticking probabilities $\langle S_0^{\rm H_2, HD, D_2} \rangle (T)$, adsorption energies $E_0^{\rm H_2, HD, D_2}$ as well as reactant $Q_{\rm H^*, D^*}$ and product $Q_{\rm H_2, HD, D_2}$ partition functions.

$$k_{\rm H_2}(T) = \langle S_0^{\rm H_2} \rangle (T) \sqrt{\frac{k_{\rm B}T}{2\pi m_{\rm H_2}}} \frac{Q_{\rm H_2}/V}{(Q_{\rm H^*}/A)^2} \exp\left(-\frac{E_0^{\rm H_2}}{k_{\rm B}T}\right).$$
 (1)

The QRM rate constant for H_2 desorption by the recombination of two adsorbed H atoms, $k_{H_2}(T)$, given by Eq. (1), is derived from the principle of detailed balance in Section S5 (a) of the SM. Expressions for $k_{HD}(T)$ and $k_{D_2}(T)$ were easily obtained by analogy. Accurate values for $E_0^{H_2,HD,D_2}$ and $\langle S_0^{H_2,HD,D_2} \rangle(T)$ can be obtained from prior experiments (Section S3 and S6, SM). These measured quantities allowed us to avoid errors associated with the theoretical determination of the thermal dissociative adsorption rates and Density Functional Theory (DFT) calculations of adsorption energies, which can be highly dependent on the choice of exchange-correlation functional (21). In addition, the partition function for the hydrogen molecule in the gas phase Q_{H_2} is well known.

The adsorbate partition functions Q_{H^*,D^*} are crucial inputs to the QRM and were computed with a Quantum Potential Energy Sampling (QPES) method, where the nuclear part of the partition function is obtained by a direct state count. States and energies were obtained by solving the nuclear Schrödinger equation with DFT interaction potentials computed with two different functionals and assuming a static Pt surface (Section S1 (b), SM). This procedure was performed for H interacting with both Pt(111) and (332). We found that Q_{H^*} is weakly dependent on the choice of DFT functional (Section S5 (e), SM). The electronic contribution to Q_{H^*} , which accounts for the two-fold spin-degeneracy of H-Pt system, was explicitly included.

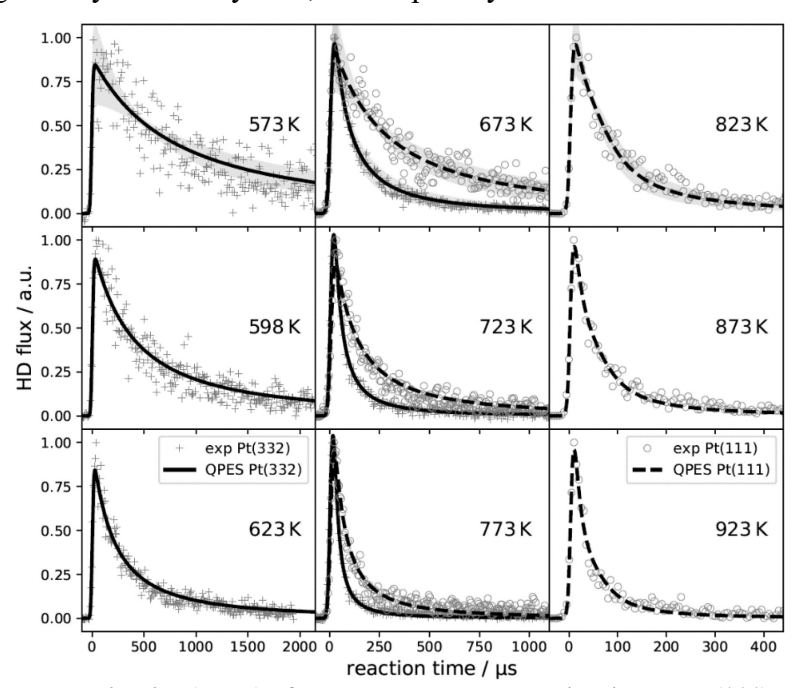


Figure 1: Velocity resolved kinetics (VRK) of hydrogen atom recombination on Pt(111) and Pt(332). (a) Measured HD formation rates for Pt(111)(\circ) and Pt(332) (+) are compared to the results of the QRM (dashed and solid lines). The temperature dependence and the transient rate of the measurements is quantitatively captured by the model

for both facets. The shaded regions of the top three panels indicate 2σ -uncertainty, mainly associated with the absolute reactant flux measurement (~30%) and the dissociative adsorption energies. The excellent agreement between VRK and QRM is achieved without adjustable parameters.

Figure 1 presents the experimentally obtained HD formation rates for reaction on Pt(111) and Pt(332) and compares them to a simulation of the experiment. The simulations used rate constants from the QRM for all three isotopologues (Fig. S9, SM) and accounted for the temporal profile of the dosing pulse and its spatial inhomogeneity, f(t,r) (Fig. 2 (a)) as well as reactant diffusion. This aspect of the data analysis goes beyond past work and is essential, because the rates of 2^{nd} order reactions are sensitive to surface concentration distributions and gradients. The full diffusion-reaction model is described in Section S7 (SM) and accounts for well-known diffusion effects on surface reaction rates discussed in previous work (22). Figure 2 (b) shows that the isotope effect at these temperatures is small and well described by the QRM. Inspection of Fig.'s 1 and 2 (b) clearly shows that the QRM, which has no adjustable parameters, reproduces experiment for reactions on both Pt(111) and (332).

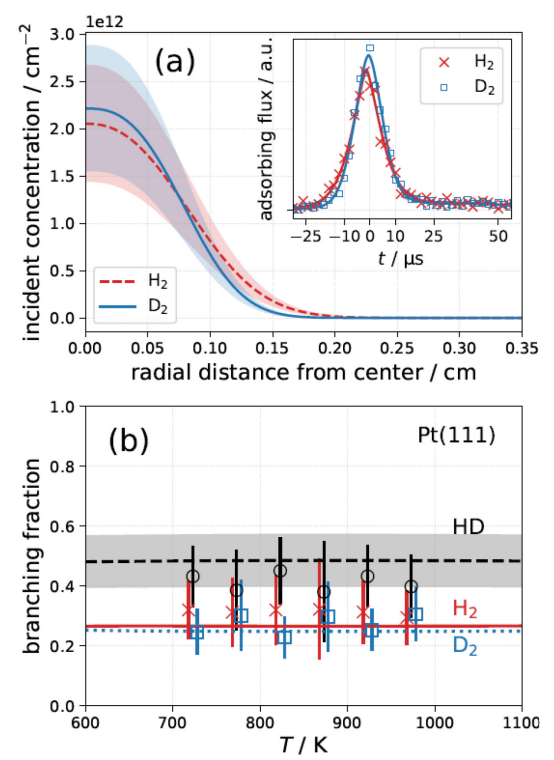


Figure 2: Calibration of the molecular beam and isotopic branching (a) The time and space dependent H_2 and D_2 dosing profiles used to determine the absolute initial concentration of H^* and D^* . These results were obtained from laser based calibration of the molecular beam flux and are required to accurately determine the recombination rate constants. (b) Isotopic branching fraction from Velocity Resolved Kinetics (VRK) experiments (symbols) and QRM (lines). The error bars and the grey shaded region reflect 2σ uncertainty in the experiment and model, respectively. Note that some symbols have been shifted by ± 5 K for clarity.

Figure 3 shows the VRK derived H* recombination rate constants (black circles) compared with previous work (red trapezoids) for reaction on Pt(111). Previous studies used Temperature Programmed Desorption (TPD) for T < 400 K (23-26) and molecular beam relaxation spectrometry (MBRS) for T > 400 K (27, 28). The uncertainty in the previously reported rate constants spans three orders of magnitude. We note that previous work studied different isotopic recombination reactions (Fig. S8); however, given the small isotope effect found in the present study (Fig. 2 (b) and Fig. S9), these differences between experiment cannot explain the large range of reported values. The VRK measurements clearly distinguish the accuracy of two previous MBRS measurements falling within the uncertainty range of Ref. (27), but differing by two orders of magnitude from rate constants reported in Ref. (28).

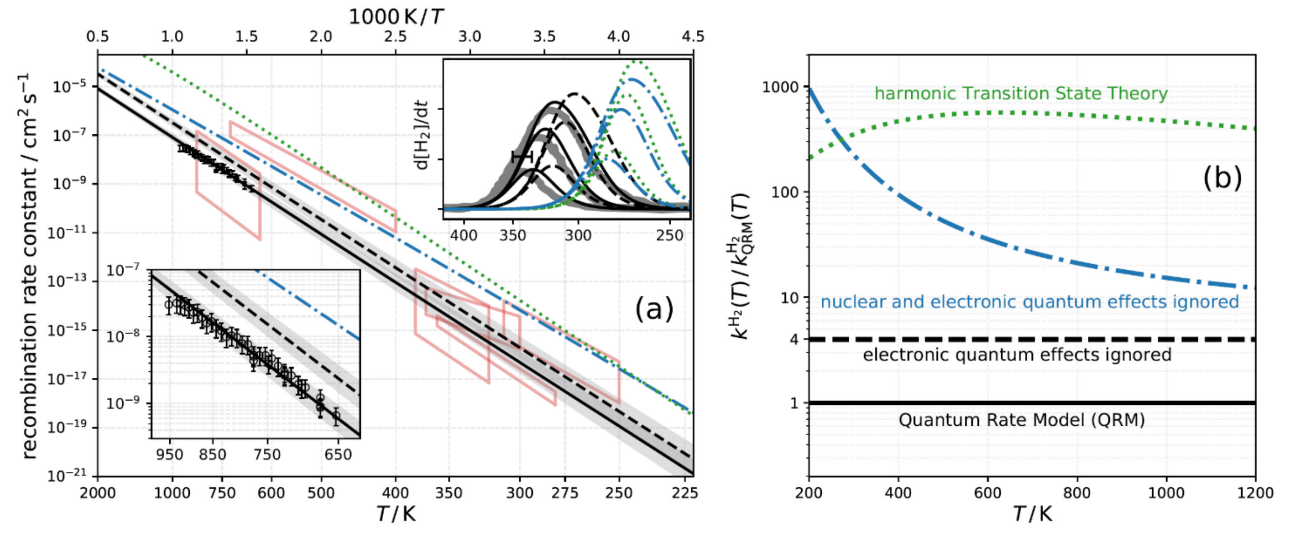


Figure 3: Rate constants for H atom recombination on Pt(111). (a) Red trapezoids show the temperature range and rate constant uncertainties of previous work (23-28) – see text. Experimental results from this work (o) with 2σ-error bars compared to the results of: the QRM (black solid line), hTST (green dotted line), CRM (blue dash-dotted line) and QRM neglecting electron spin (black dashed line). Lower inset shows an expanded view. The upper inset compares TPD spectra (broad grey lines) from Ref. (29) to the predictions of the QRM model, QRM neglecting spin, the CPES model and the hTST model for three initial H* coverages of 0.1, 0.2 and 0.3 ML. The grey shaded region and the horizontal error bar on one of the modeled TPD spectra reflects the uncertainty of the experimental H₂ chemisorption energy. The ability of the QRM rate-constants to quantitatively reproduce experiment demonstrates the importance of both nuclear and electronic quantum effects. (b) Comparison of three approximate rate models' predictions to QRM rate constants. Neglecting spin-degeneracy, employing a fully classical approximation or using a commonly adopted approximate quantum model all introduce large errors even at high temperatures. Similar errors are seen for recombination rates on the stepped Pt(332) surface – see Fig. S14. See Fig. S12 in the SM for detailed decomposition of the errors observed from hTST and adsorbate entropy approximations.

A hallmark of a fundamentally correct model is its ability to reproduce accurate experimental data over a broad temperature range. The QRM employs a fundamentally correct *ab initio* adsorbate partition function leading to excellent agreement with experiment over a large temperature

range. The performance of the QRM for Pt(111) at temperatures between 650 and 950 K is demonstrated by comparison to VRK-derived rate constants, whereas low temperature comparisons rely on TPD. Uncertainties in the TPD-derived rate constants arise from: questionable approximations used to derive rate constants from the data, neglect of the coverage dependence of adsorption energies (26), dubious estimations of pre-factors (25) and neglect of the influence of steps (23). To make the most meaningful comparison, we have used the QRM to directly simulate TPD spectra from Ref. (29), where the influence of steps was carefully identified and removed (Sec. S8, SM). Here, we also accounted for the previously reported coverage dependence of the adsorption energy (24, 30) (Sec. S6 and Fig. S11, SM). The comparison is shown in the upper inset of Fig. 3 (a). The solid black lines of the QRM are in excellent agreement with the TPD spectra (broad gray lines, from Ref. (29)) for three initial coverages.

The aforementioned comparisons to kinetics experiments carried out between 250 and 950 K, demonstrated the validity of the QRM rate constants over twelve orders of magnitude and for hydrogen atom coverages up to 0.3 ML. Within the context of the principle of detailed balance as implemented in the QRM, this coherent picture demonstrates the quantitative consistency of previously reported sticking coefficients and binding energies with the kinetics measurements of this work. The agreement over such a wide range of rates provides confidence in the QRM rate constants, making hydrogen recombination on Pt(111) a reliable benchmark for approximate rate theories in surface chemistry.

It is worth noting that the QRM as implemented in this work is semi-empirical as it relies on experimental values of thermal sticking coefficients and adsorption energies. However, it also provides a path to an *ab initio* theory of thermal reaction rates, if these quantities can be accurately calculated from first principles.

The framework of the QRM allows us to critically test the quality of predictions based on approximations commonly used in kinetic modeling of heterogeneous catalysis. The results of this analysis are shown in Fig. 3. The most widely used model for rate constants (hTST) introduces quantum effects in an approximate way, where nuclear partition functions are computed assuming separable motion into contributing degrees of freedom that can each be approximated as harmonic oscillators. By definition, re-crossing corrections are not included in hTST (12, 13). The hTST rate constant, calculated by placing the dividing surface far above the surface, are shown as a green dotted line in Fig. 3. This approximation overestimates the experimental reaction rate constant by

two to three orders of magnitude at all temperatures between 200 and 1200 K. The major source of errors in hTST arise from the harmonic simplifications made to the H-Pt interaction potential (resulting in errors of a factor 5-25) and the neglect of re-crossing corrections to TST (with errors of a factor 5-10)—see Fig. S12 (a) in the SM for details.

The next more sophisticated level of rate theory uses the Complete Potential Energy Sampling (CPES) method to characterize entropy associated with H*'s in-plane degrees of freedom. CPES is considered by many to provide the most accurate adsorbate partition function (31) and it has been applied to characterize H interaction at metals (11). It accounts for anharmonicity by using a semi-classical partition function computed from the adsorbate potential energy surface, which may be obtained with DFT (11, 14, 31). To evaluate this approach, we modified the QRM, replacing the QPES by the CPES adsorbate partition function, but retaining the other parameters in Eq. (1). This substitution serves to illustrate the classical counterpart of the QRM, which we hereafter denote as the CRM. The rate constants predicted by the CRM are shown as blue dash-dotted lines in Fig. 3. The CRM performed better than hTST, but nevertheless overestimated the rate constant by a factor of 20, even at temperatures as high as 1000 K. The error is more than 100-fold at 300 K, a temperature typical for electrochemical applications. Although our detailed analysis is focused on Pt(111), the errors introduced by hTST and the CRM are similar for reactions on Pt(332) (Fig. S14, SM).

A major source of error in the CPES method arises from classical description of the adsorbate's in-plane motion. This can be understood by considering that the in-plane zero-point energy (ZPE) of H* on Pt(111) (58 meV) is almost equal to the classical diffusion barrier (60 meV)—see Fig. S13, SM. Thus, classical and quantum description of H* motion on the surface lead to very different results. CPES excludes H* from classically forbidden regions of space, whereas quantum mechanically there is a significant probability to populate these regions. Furthermore, CPES does not account for the uncertainty principle, which prevents localization of H* at the classical energy minimum at low temperature. The surface area explored by the H-atom is underestimated by CPES and thus, so too is the adsorbate entropy. This results in an overestimate of the corresponding rate constant. Our results underscore the importance of quantum delocalization and help explain why the deviations of CRM become more severe at low temperatures. Quantum delocalization is also the reason why hTST fails. All quantum states above the ground state exhibit probability maxima at positions far from the potential energy minimum—Fig. S13, SM.

We may investigate other sources of error in the CRM by using the QPES partition function, but neglecting electron spin. Figure 3 (a) shows rate constants predicted on this basis and in Figure 3 (b), one can see that neglect of electron spin-degeneracy led to a 4× overestimate of the rate constant at all temperatures. This result can be understood intuitively if we that when two H* atoms attempt to react, they must approach one another in one of four degenerate states with either parallel (triplet) or antiparallel (singlet) spins. Only the singlet state correlates with the formation of gas-phase singlet H₂ products; hence including spin-degeneracy reduces the reaction rate by a factor of four. This result should not come as a surprise to those familiar with rate calculations for gas-phase reactions where spin-degeneracy is routinely included (1). Nonetheless, to the best of our knowledge, this is the first demonstration that the rates of thermal reactions at metal surfaces depend on adsorbate spin.

The QRM developed in this work also describes the reaction rate on stepped surfaces. In Fig. 4 (a), we compared the predicted rate constants of the QRM for Pt(111) and (332) surfaces to those derived from VRK experiments. For details of the QRM treatment of the reaction on Pt(332), see Section S1(b) and S6 (SM). Experiment shows that near 700 K, the rate constants for reaction on the (332) facet is larger than that on the (111) facet, an effect that is quantitatively captured by the QRM. This result may appear surprising, because the H atom's binding energy is larger at steps than at terraces (30, 32). A naïve view of Eq. (1) suggests this leads to a lower rate constant. However, careful analysis of the thermally populated quantum states used in the QPES partition functions showed that at these temperatures, H atoms on the (332) facet tend to remain localized near step sites (Fig. S15, SM). This fact reduces their in-plane translational entropy and leads to an increase in the rate constant as the effect of entropy is larger than that produced by a larger step binding energy.

This observation reflects how changing temperature alters the relative influence of energy and entropy on the rate constant. In past work, similarities in TPD spectra of H_2 desorbing from Pt(111) and a B-type stepped Pt surface at $T \sim 350$ K were taken as evidence for a lack of preferential step binding (26). Inspection of QRM rate constants in Fig. 4 (a) reveals that at 350 K, the similarity in desorption rate constants arises from compensation between energetic and entropic contributions see Sec. S8 (SM) for details. Our work supports conclusions derived from helium atom and ion scattering experiments that H binds more strongly to B-type steps (30, 32). Only at much lower

temperatures does the energetic preference for H binding at steps cause the rate constant on the stepped surface to drop below that on (111) terraces.

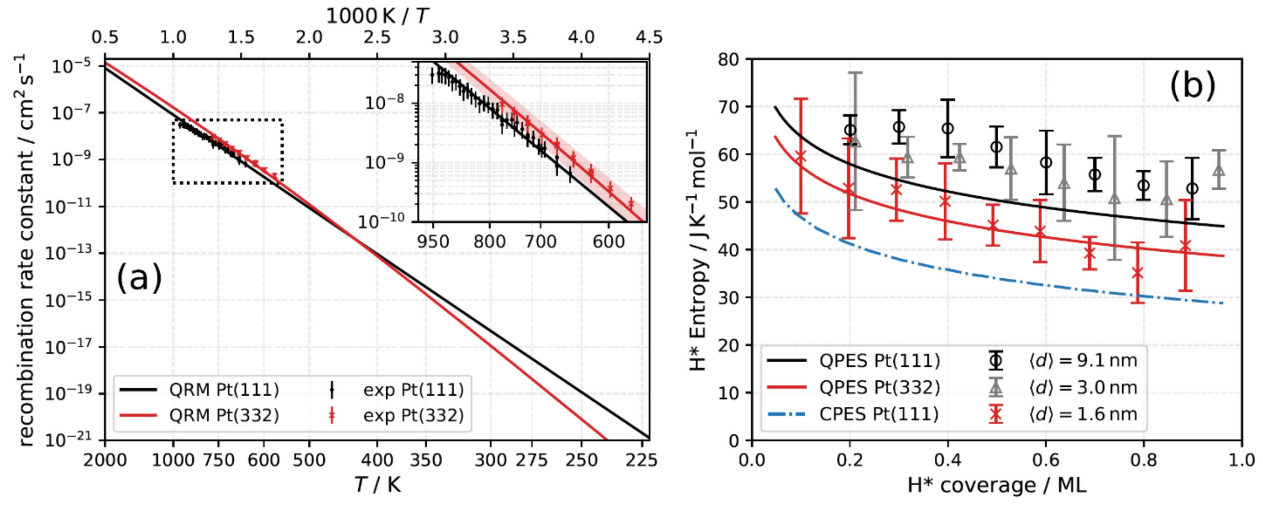


Figure 4: The influence of steps on H atom recombination on Platinum. (a) Rate constants derived from VRK experiments (symbols) for hydrogen atom recombination on Pt(111) and Pt(332) are compared to QRM predictions (solid lines). The 2σ uncertainty of Pt(332) QRM's rate constants is shown as a red shaded region. (b) Entropies obtained experimentally at 598 K (symbols with 2σ -errorbars) and from CPES (dash-dotted blue line) for H* bound to Pt nanoparticles from Ref. (11). QPES entropies for H* bound to Pt(111) (solid black line) and Pt(332) (solid red line) obtained in this work – see Sec. S9 (SM). The nuclear quantum effect contribution is 12 J mol⁻¹ K⁻¹ and that of electron spin is 6 J mol⁻¹ K⁻¹. The comparison suggests that the nanoparticle-size dependence of the H* entropy is determined by the concentration of steps.

Because the QRM approach developed in this work provides an accurate determination of rate constants on stepped surfaces, we expect that QPES entropies used in the QRM would help us understand experiments performed on size-selected Pt nanoparticles (11), because smaller nanoparticles exhibit higher step-concentrations. Figure 4(b) shows measured H* entropies for Pt nanoparticles of various sizes reproduced from Ref. (11) – the entropy increases with the nanoparticle size, consistent with observations presented above that Pt steps reduce H* entropy. Also shown are CPES entropies reported in Ref. (11), which fail to describe entropies derived from experiment. Remarkably, the entropies found using the QPES method for H* bound to Pt(111) (see Fig. 4(b)) are in good agreement with entropies for the largest particle sizes. Note that surfaces of large nanoparticles are primarily composed of the (111) facets (11). Figure 4(b) also shows QPES entropies for H* on the (332) facet, which compare well to experimentally obtained entropies on small nanoparticles. This comparison further supported our hypothesis that the H* entropy decreases as nanoparticle size decreases and the relative importance of step defects increases. This result points out the importance of quantum effects even for the description of thermodynamic state functions in advanced catalytic materials.

In conclusion, this work has shown, H* recombination on Pt surfaces exhibits large quantum

effects even at elevated temperatures relevant to catalysis. These quantum effects in the reactions

rates and in thermodynamic properties of the adsorbed H atoms arise in part from the H atom's

light mass, where a careful treatment of its wave properties is required to obtain accurate results.

Such nuclear quantum effects will diminish in importance for heavier systems. However, the effect

of spin-degeneracy demonstrated here will remain of general importance for a host of reactions of

heavier species involved in real-world catalysis. It is currently not easily possible to determine the

lowest energy spin-state for metal surfaces with DFT. Developing theoretical and experimental

methods able to probe the general influence of spin on reaction rates presents the next challenge

on the way towards fully predictive surface chemistry at metal catalysts.

Corresponding Authors

* Dmitriy Borodin: dborodi@mpinat.mpg.de

** Alec M. Wodtke: alec.wodtke@mpinat.mpg.de

Author Contributions

The manuscript was written through contributions of all authors. All authors have given approval

to the final version of the manuscript.

Acknowledgments

We thank Prof. John C. Tully for helpful discussions. **Funding:** D.B. and M.S. thank the BENCh

graduate school, funded by the DFG (389479699/GRK2455). T.N.K., G.S., A.K., M.S. and J.F.

acknowledge support from the European Research Council (ERC) under the European Union's

Horizon 2020 research and innovation program (grant agreement no. [833404]). Y. W., J. Z., and

H. G. acknowledge the U.S. National Science Foundation (Grant. No. CHE-1951328) and H. G.

thanks the Alexander von Humboldt Foundation for a Humboldt Research Award. The calculations

11

were partially performed at the Center for Advanced Research Computing (CARC) at UNM and

at National Energy Research Scientific Computing (NERSC) Center. Author contributions: DB,

MS and JF conducted the transient kinetics experiments. Flux calibration procedures were devel-

oped by DB, GBP, MS, FN, DJA and TNK. DB and DS developed the reaction-diffusion analysis.

DB and AMW developed the quantum rate model. NH, YW, JZ and HG conducted DFT calcula-

tions. DB, NH, AK and HG analyzed DFT calculations and developed methods for description of

nuclear partition functions. MS, JF, GS, TNK, DJA, DS and AK participated in discussion of the

results. DB, DJA, HG, and AMW wrote the manuscript and the supporting material. All authors

contributed to the reviews of the manuscript and the supporting material. Competing interests:

None declared. Data and material availability: All data needed to evaluate the conclusions in

the paper are present in the paper or the supplementary materials and are publicly available in the

repository (33).

Supplementary Materials

Materials and Methods

Supplementary Text

Figs. S1 to S15

References (34-71)

12

REFERENCES

- 1. J. L. Bao, D. G. Truhlar, Variational transition state theory: theoretical framework and recent developments. *Chem. Soc. Rev.* **46**, 7548-7596 (2017).
- 2. F. Studt, Grand challenges in computational catalysis. *Front. Catal.* 1, 1-4 (2021).
- 3. A. H. Motagamwala, J. A. Dumesic, Microkinetic modeling: A tool for rational catalyst design. *Chem. Rev.* **121**, 1049-1076 (2021).
- 4. J. E. Sutton, W. Guo, M. A. Katsoulakis, D. G. Vlachos, Effects of correlated parameters and uncertainty in electronic-structure-based chemical kinetic modelling. *Nat. Chem.* **8**, 331-337 (2016).
- 5. G. B. Park *et al.*, The kinetics of elementary thermal reactions in heterogeneous catalysis. *Nat. Rev. Chem.* **3**, 723-732 (2019).
- 6. P. Sabatier, *Catalysis in Organic Chemistry*. (D. Van Nostrand Company, New York, 1922).
- 7. G. Ertl, Reactions at surfaces: From atoms to complexity. *Angew. Chem. Int. Ed.* **47**, 3524-3535 (2008).
- 8. A. Godula-Jopek, *Hydrogen Production by Electrolysis*. (Wiley-VCH, 2015).
- 9. M. P. D'Evelyn, R. J. Madix, Reactive scattering from solid surfaces. *Surf Sci Rep* **3**, 413-495 (1983).
- 10. Y. V. Suleimanov, F. J. Aoiz, H. Guo, Chemical reaction rate coefficients from ring polymer molecular dynamics: Theory and practical applications. *J. Phys. Chem. A* **120**, 8488-8502 (2016).
- 11. M. García-Diéguez, D. D. Hibbitts, E. Iglesia, Hydrogen chemisorption isotherms on platinum particles at catalytic temperatures: Langmuir and two-dimensional gas models revisited. *J. Phys. Chem. C* **123**, 8447-8462 (2019).
- 12. S. Bhandari, S. Rangarajan, C. T. Maravelias, J. A. Dumesic, M. Mavrikakis, Reaction mechanism of vapor-phase formic acid decomposition over platinum catalysts: DFT, reaction kinetics experiments, and microkinetic modeling. *ACS Catal* **10**, 4112-4126 (2020).
- 13. M. Jørgensen, H. Grönbeck, First-principles microkinetic modeling of methane oxidation over Pd(100) and Pd(111). *ACS Catal* **6**, 6730-6738 (2016).
- 14. A. Bajpai, P. Mehta, K. Frey, A. M. Lehmer, W. F. Schneider, Benchmark first-principles calculations of adsorbate free energies. *ACS Catal* **8**, 1945-1954 (2018).

- 15. D. Borodin *et al.*, Kinetics of NH₃ desorption and diffusion on Pt: implications for the Ostwald process. *J. Am. Chem. Soc.* **143**, 18305-18316 (2021).
- 16. J. Neugebohren *et al.*, Velocity-resolved kinetics of site-specific carbon monoxide oxidation on platinum surfaces. *Nature* **558**, 280-283 (2018).
- 17. R. van Lent *et al.*, Site-specific reactivity of molecules with surface defects-the case of H₂ dissociation on Pt. *Science* **363**, 155-157 (2019).
- 18. A. C. Luntz, J. K. Brown, M. D. Williams, Molecular beam studies of H₂ and D₂ dissociative chemisorption on Pt(111). *J. Chem. Phys.* **93**, 5240-5246 (1990).
- 19. K. Tonokura, T. Suzuki, Slicing photofragment spatial-distribution by laser sheet ionization. *Chem. Phys. Lett.* **224**, 1-6 (1994).
- 20. C. R. Gebhardt, T. P. Rakitzis, P. C. Samartzis, V. Ladopoulos, T. N. Kitsopoulos, Slice imaging: A new approach to ion imaging and velocity mapping. *Rev. Sci. Instrum.* **72**, 3848-3853 (2001).
- 21. G. J. Kroes, Computational approaches to dissociative chemisorption on metals: Towards chemical accuracy. *Phys Chem Chem Phys* **23**, 8962-9048 (2021).
- 22. D. R. Olander, Heterogeneous chemical kinetics by modulated molecular beam mass spectrometry. *J. Colloid Interface Sci.* **58**, 169-183 (1977).
- 23. K. Christmann, G. Ertl, T. Pignet, Adsorption of hydrogen on a Pt(111) surface. *Surf. Sci.* **54**, 365-392 (1976).
- 24. B. Poelsema, K. Lenz, G. Comsa, The dissociative adsorption of hydrogen on defect-'free' Pt(111). *J. Phys. Condens Matter* **22**, 304006 (2010).
- 25. P. Samson, A. Nesbitt, B. E. Koel, A. Hodgson, Deuterium dissociation on ordered Sn/Pt(111) surface alloys. *J. Chem. Phys.* **109**, 3255-3264 (1998).
- 26. M. J. van der Niet, A. den Dunnen, L. B. Juurlink, M. T. Koper, The influence of step geometry on the desorption characteristics of O₂, D₂, and H₂O from stepped Pt surfaces. *J. Chem. Phys.* **132**, 174705 (2010).
- 27. G. E. Gdowski, J. A. Fair, R. J. Madix, Reactive scattering of small molecules from platinum crystal surfaces: D₂CO, CH₃OH, HCOOH, and the nonanomalous kinetics of hydrogen atom recombination. *Surf. Sci.* **127**, 541-554 (1983).
- 28. M. Salmerón, R. J. Gale, G. A. Somorjai, A modulated molecular beam study of the mechanism of the H₂–D₂ exchange reaction on Pt(111) and Pt(332) crystal surfaces. *J. Chem. Phys.* **70**, 2807-2818 (1979).
- 29. S. K. Jo, Weakly-bound hydrogen on defected Pt(111). Surf. Sci. 635, 99-107 (2015).

- 30. B. J. J. Koeleman, S. T. de Zwart, A. L. Boers, B. Poelsema, L. K. Verhey, Adsorption study of hydrogen on a stepped Pt(997) surface using low energy recoil scattering. *Nucl. Instrum. Methods Phys. Res.* **218**, 225-229 (1983).
- 31. M. Jørgensen, H. Grönbeck, Adsorbate entropies with complete potential energy sampling in microkinetic modeling. *J. Phys. Chem. C* **121**, 7199-7207 (2017).
- 32. B. Poelsema, G. Mechtersheimer, G. Comsa, The interaction of hydrogen with platinum (S)[9(111)x(111)] studied with helium beam diffraction. *Surf. Sci.* **111**, 519-544 (1981).
- 33. D. Borodin, Hydrogen atom recombination on Pt(111) and Pt(332). Zenodo, (2022).